# Analysis of Spacecraft Propellant Plumes in the GEO Plasma Environment

**Adrienne Rudolph**
*University of Maryland, ExoAnalytic Solutions, Inc.*
**Phillip Cunio, Marcus Bever, Christopher Bolig, and Douglas Hendrix**
*ExoAnalytic Solutions, Inc.*
**Stuart Eves**
*SJE Space Ltd.*

## ABSTRACT

ExoAnalytic Solutions (Exo) uses their global space surveillance telescope network to track large delta-V orbit insertions, among other ongoing activities in the vicinity of Geosynchronous Earth Orbit (GEO). The propellant plumes of a select group of spacecraft during their respective insertion maneuvers have been found to exhibit behaviors that appear to indicate plasma effects are dominating the physics of said plumes. This paper addresses the plasma environment at GEO and its interaction with propellant plumes through image analysis and by modeling plumes using rocket nozzle design theory under an ideal, non-ionized gas assumption. The results of this study yield that plume development likely relies on a mixture of various propulsion and plasma environment properties, and that conical plumes can be reasonably modeled as neutral non-ionized gasses, unless accompanied by an amorphous cloud. Understanding the fundamentals will allow for more precise magnetohydrodynamic modeling with varying levels of ionization, where data on known propulsions systems, thruster plume video sequences, and measurements of the plasma environment will be used to estimate the accuracy of the model.

## 1. INTRODUCTION

Investigations of how spacecraft interact with the space environment have remained ongoing for decades, and continue to be essential in understanding how spacecraft exhaust plumes react to the plasma environment surrounding the earth. Plumes are defined by the exhaust products that are deposited into the surrounding environment that persist near, around, or behind the associated space vehicle [3]. This is particularly important in the field of space situational awareness insofar as it may allow remote sensors to discern facts about space objects and their behaviors. The characteristics of a propellant plume may display features that uniquely indicate the type of maneuver a spacecraft has performed or the specific propellants on board. Furthermore, the manner in which spacecraft plumes move and disperse may also reveal properties of the atomic species present in the local space environment. Because in-situ measurements may not always be available, it is necessary to be able to classify plumes using ground-based observations. ExoAnalytic Solutions (Exo) specializes in space situational awareness, inclusive of knowing, predicting, and characterizing the movement of space vehicles at Geosynchronous orbit (GEO). Telecommunications, remote sensing, and other types of satellites existing at GEO are vital to modern life and must be monitored, protected, and well understood.

Images captured by Exo's ground-based global telescope network captured three different satellites performing a series of high delta-v maneuvers that emitted plumes which embody three main characteristics that differ from the more commonly observed hemisphere-like plumes (Fig. 1): a long duration, a conical shape, and a maintained static form as if constrained by invisible boundaries (Fig. 1). Research would suggest these plumes are created by highly impulsive injection burns or propellant dumps with rapid expansion and exchange of charges between the associated plumes and the ambient plasma environment. Such evidence leads to the hypothesis that the uncommon behavior may be influenced by the plasma environment at GEO and it may be possible to classify the plumes given they all exist in the same environment. Researchers have consistently probed well known related problems such as spacecraft surface charging caused by the influx of hot plasma in the magnetosphere, and the coating of spacecraft with material-degrading gasses by expelled propellant from second stage thrusters [16, 17]. However, the characterization of a spacecraft's expelled propellant plumes and how they interact with, or are likewise affected by, surrounding plasma in the space environment has been studied to a lesser extent.

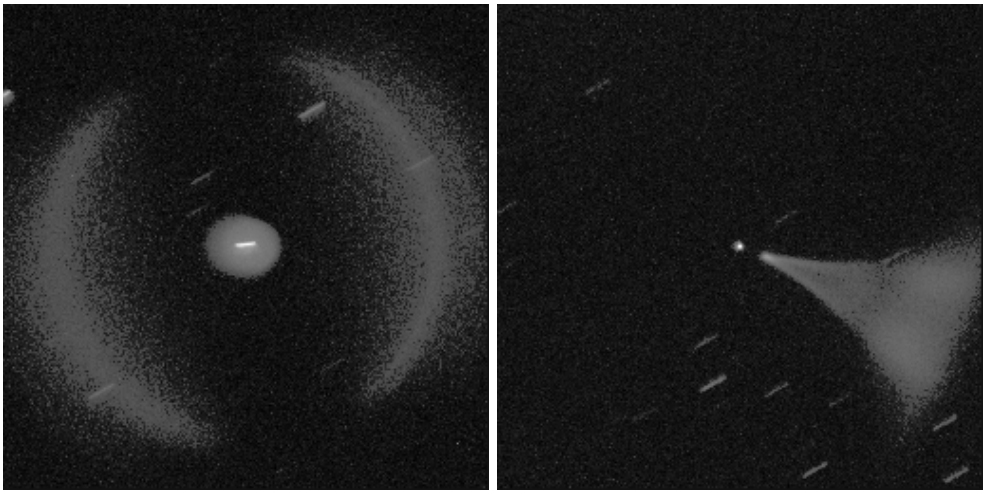

Fig 1. Hemispherical Plume (left) and Conical Plume (right) Observed by Exo Telescopes

The main technical focus of this effort is modeling and simulating the observed propellant plumes, thereby paving the way for more advanced analyses using magnetohydrodynamic (MHD) codes and a future estimate of the degree to which the observed plumes fit the models for varying degrees of ionization. Qualitatively, this work seeks to understand how a specific propellant, or combination of propellants, can interact with the plasma environment at GEO to produce the visual results of long-lived, shape-maintaining propellant plumes from spacecraft performing orbital insertion burns. Knowledge of the effects of the plasma environment on propellant plumes can prove instructive in the effort to characterize objects at GEO for which we have incomplete information. By anchoring the results of our simulations with observations, it may be possible to determine what effects are likely to occur for various types of expended propellant in the charged environment at GEO and to eventually aid in the identification of the fuels and oxidizers used by spacecraft for which the propellant types are unknown. It may also aid in identifying key generators of the differences between hemispherical and conical plumes.

## 2. BACKGROUND

Previous research examines the effects of spacecraft thruster plumes on the surrounding space plasma environment. One in-situ study observed neutral gas injections by the Cygnus spacecraft, finding that impulsive firing of thrusters may excite waves within the plasma at low-Earth-orbit (LEO) and have a strong effect on the frequency of the wave emissions [2]. This frequency, or plasma frequency, is the frequency at which electrons within the plasma naturally oscillate relative to the ions in the plasma. A change in the ion composition, density, and temperature can be affected by the injection of exhaust from satellites, more specifically, by a charge exchange among the ambient oxygen ions in the ionosphere and the combusted products from the rocket [2]. This change in plasma frequency can be characterized by observable changes in radio frequency (RF) emissions from the volume of space near the plume emission site. These RF measurements can show the existence and strength of changes, but are not necessarily able to map plasma-plume interaction spatially.

Another study focused on maneuvers made by the Space Shuttle Endeavor in LEO, where large fluxes of plasma were observed being generated by an increase in ion current as a result of the interaction between the thruster plumes and the ambient space environment. These interactions were also found to generate regions of high-density plasma [5]. The ion plume signals, measured by the Canary electrostatic analyzer instrument aboard the ISS, were detected as current. Utilizing unsteady Monte Carlo and Particle-In-Cell (PIC) analyses that employed charge exchange cross section data and a magnetic field model, simulated local plasma characteristics and their associated ion currents were produced; these demonstrated a strong correlation with the ion current signals in the empirical plume data [5]. This implies the resulting unsteady simulations of the research were in strong agreement with current and plasma density measurements.

The results of the two studies are very similar in that they both find the creation and disruption of plasmas in the local space environment to be caused by the firing of spacecraft thrusters. While the results are significant in understanding interactions of propellant plumes in the plasma environment, four key factors must be considered

differently for this particular investigation: interaction type (plume-to-plasma vs plasma-to-plume), altitude, duration, and propellant type. This research seeks to understand how the surrounding space plasma environment affects the characteristics (i.e., size, shape, duration) of the plumes being expelled, and if other factors should be considered. Additionally, the previous studies performed calculations based on known properties of the ionosphere at LEO, whereas our observations rely on properties of the plasmasphere and ion composition at GEO. The plasma environments in these two space domains are not necessarily the same. Two additional studies examining rocket plume expansions at GEO do in fact analyze similar properties as this work, where both investigate the interactions of spacecraft plumes and the magnetosphere.

The first study models steady and unsteady plume types from hydrazine chemical rocket thrusters using the direct simulation Monte Carlo (DSMC) and PIC methods, tools that help model charge exchange collisions between the combusted thruster plume species and the ambient ions at GEO [14]. Results of this study indicate that the hydrazine plumes are formed by the depletion and replenishing of local ambient ions via charge exchanges, where the ion plumes are less dense than neutral plumes because the nature of the hydrogen ions becomes depleted by the charge exchange collisions [14]. To a partial extent, photoionization processes were discovered to increase the plasma density in the immediate vicinity of the spacecraft as well as ionize the highly dense plume (relative to the ambient environment) at the thruster exit [14]. Results from the models show that there are differences in the plume expansions based on their level of neutrality (or ionization), where neutral plumes were found to typically expand in only one direction - directly away from the source, and ionized plumes could be found both upstream and downstream of the thruster. Further results indicate that local electrostatic forces have a strong influence on the charged chemical species released in the propellant and consequently, the formation and behavior of the ion plumes. In essence, a spacecraft thruster is found to eject high density neutral plumes that expand into the local space environment where they interact with ambient hydrogen ions that, through some level of charge exchange, form subsequent ion plumes [14].

The second study performs a similar analysis on hydrazine plumes, with the exception of simplified assumptions, such as no charge exchange collisions, free molecular flow, and neglecting the photoionization effects on the combusted product $H_2$ to model thruster firings of neutral plumes at 0.1 seconds (s), 1.4 s, and 9.9 s as they expand into the magnetosphere [12]. The results of the research were numerically and analytically calculated time-dependent flow properties for three station-keeping maneuvers [12]. Congruent with the previous analysis [14], analytical results indicate that due to diffusion, the peak number densities of the plumes reduce by a large factor the further they move from the thruster [12].

While these analyses are beneficial for better characterizing neutral plume properties, which are also analyzed in this work, our investigation primarily lies in understanding the flow properties and interactions of the uncommon, conical plumes that have been observed to persist for substantially longer durations than the simulated plumes in previous studies, and how the conical and hemispherical plumes differ in both formation and expansion. Furthermore, each of the works previously mentioned examine spacecraft engines that only use hydrazine propellant, whereas the engines noted in our observations are believed to utilize liquid oxygen and liquid hydrogen in some cases as well as hydrazine in others. It is reasonable to assume that different propellant mixtures may produce different plume chemistry and consequently different ionic species, and by extension, plume behaviors [14]. It should also be noted that the primary focus of the aforementioned studies is model- or computational-based, whereas our research is rooted in observational data and real-world examples for comparison.

## 3. SPACE PLASMAS

### 3.1 The Nature of Plasmas

Before investigating how a plasma may affect propellant plumes in space, one must first understand what a plasma is and its significance within the space environment. Plasma is the fourth state of matter and is central to the topic of space weather and understanding the space environment. A plasma is a quasi-neutral gas made up of neutral and charged particles [1]. When a gas is heated to very high temperatures, on the scale of 10,000 - 100,000K (10 - 100eV) , the atoms within the gas begin to lose their electrons, leaving the electrons to fly freely about (Fig. 2)**.**

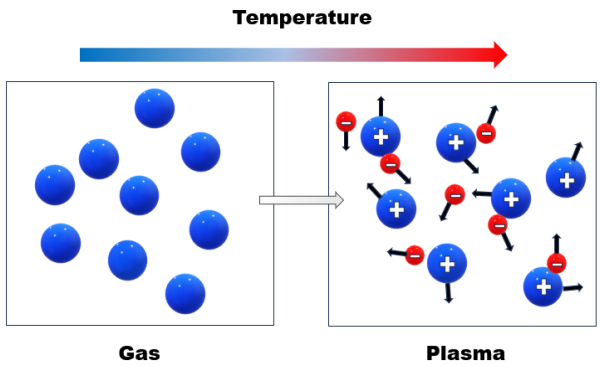


Fig. 2. Diagram of a gas transitioning to a plasma

This process is called ionization. When an atom is ionized, it will remain charged until it combines with another electron. Overall, plasmas *resemble* charged neutrality, hence the term 'quasi-neutral', but due to ionization they contain within them various local concentrations of positive and negative charges that generate electric fields [1]. When the charges move around, they also generate current, and thus, magnetic fields. The movement of charged particles within an atom is fast and chaotic, so electrons are constantly separating and recombining with ions, and the resulting electric and magnetic fields continue to form and reform, exacerbating the cycle. These properties are unique because they allow plasmas to then interact with the motion of electric and magnetic fields from other charged particles.

### 3.2 Plasmas in Space

Plasmas are estimated to make up roughly 99% of all matter in the universe, can exist in both hot and cold states, and are regularly found on Earth in the form of lightning, the Aurora Borealis, plasma balls, and even the glow within neon restaurant signs [1]. However, in the context of spacecraft in this study, it is necessary to evaluate and understand the plasma that makes up the space environment, specifically at GEO. Our sun is the source of the majority of plasma in our solar system as well as that which surrounds the earth, cocooned by the magnetosphere. It is the main cause of the solar wind and Van Allen radiation belts, as well as a driver of plasma within the magnetosphere [6]. When the sun ionizes the upper atmosphere, it excites present ions and creates plasma. The coordination of the magnetic fields and Earth's rotation are then responsible for the movement of the plasma around the planet [7].

Geostationary satellites at altitudes of approximately 36,000 km above sea level are within the outer radiation belt [8], (Fig. 3). The composition of plasma, primarily the plasma pressure, at the outer radiation belt has been measured using Van Allen Probes, and is understood to vary with time of day and fluctuations in solar activity [9].

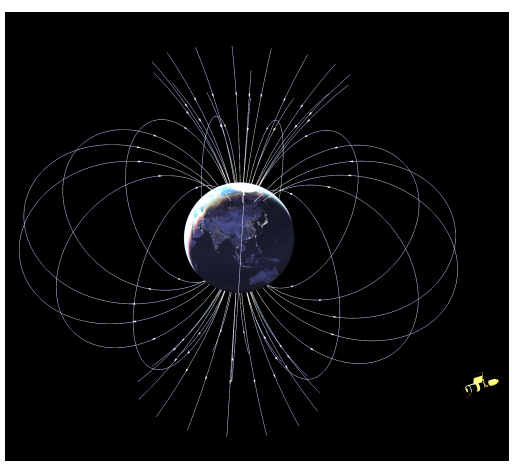

Fig. 3. Satellite at GEO with view of earth's magnetic field

The plasma pressure is a measure of the force of the particles on the bounds of the plasma they make up. The Van Allen Probes measured the plasma pressure during "quiet times," and oppositely, during periods of high geomagnetic activity. Probe data indicated that hydrogen ions ($H^+$) are both most abundant at higher altitudes and the dominant contributor to the plasma pressure during quiet times, whereas oxygen ions ($O^+$) and hydrogen ions are present at comparable levels during times of high geomagnetic activity. As geomagnetic activity continues to increase, there are clear increases in the flux of hydrogen and oxygen ions in the upper L-shells, or altitude ranges, within the outer radiation belt [9]. The composition of plasma at GEO is significant for knowing what species of particles are present, in what quantities, and at what time of day. During periods when highly dense plasma is present, it can also assist in identifying where spacecraft are likely to experience drag from plasma [4]. For this research, plasma composition provides initial insight into how the various particle species interact.

## 4. OBSERVATIONS

Exo's ground based optical sensors were tasked to observe three different geostationary satellites associated with the AFSPC-4, AFSPC-6, and USSF-8 missions (for simplicity, the satellites will be referred to by their respective mission names) during GEO orbital insertion while performing maneuvers that produced uncommon plume behavior. Most of the observed plumes originate from the upper stages of the inserting spacecraft, not necessarily the satellites themselves, although an important distinction will be discussed later. Note that plumes from other spacecraft in similar orbits were observed but not flagged for irregularities. ExoAnalytic's sensors are electro-optical sensors (Fig. 4), operating in the visible bands, that collect a new image frame of about 1 square degree approximately once every 5-10 seconds. The collected frames are processed at the collection point to identify stars and objects in the frame; stars are used to register the frames, while objects are analyzed for brightness and apparent motion, from which catalog correlation and updates are performed. When objects in the frame are identified, an image chip of 256-by-256 pixels surrounding each object is extracted, and anomalous or unanticipated behavior is identified and reported in an alert format.

Fig. 4. ExoAnalytic Solutions's Telescope Sensors

In the comparative vacuum that the space environment at GEO is, an emitted plume of thruster exhaust may be expected to expand into free space at a constant rate, with all individual particles moving at a constant velocity away from the spacecraft once emitted (with the exception of lateral interactions with other plume particles). Because the exhaust velocity of an engine is either known or a reasonably well approximated characteristic, we may expect to be able to compare the rate of motion of an element of a plume to the exhaust velocity of the whole plume, thereby assessing whether fluid dynamics exclusively are the driving force. The first subsection will discuss the properties of neutral gas dynamics, the next subsection will reveal the hemispherical plumes that were observed and briefly discuss their behavior. The following subsection will then address the observed conical plumes from each satellite, providing examples of necessary calculations for the plume expansion velocity and area. It is important to briefly review these parameters in regard to both pixel and physical space.

### 4.1 Known Neutral vs Ion Plume Behavior

Neutral plume species react to the ambient space environment, filled with various neutral, positive, and negatively charged particles, in many different ways. A neutral gas contains a stable configuration of electrons, but is subject to collisions with nearby particles through either elastic or inelastic means. Elastic collisions result in an exchange of kinetic energy from one particle to another. Inelastic collisions, like ones that occur often in the space environment, transform the kinetic energy into something else [18]. The energy can cause electrons to reach an excited state, moving up in energy levels, and sometimes be kicked off completely, resulting in ionization of what once were neutral atoms [18]. The resulting energy of excitation can also be a cause of radiation in the form of light, which will be discussed more in depth in a later section. Charge exchange, another transformation of kinetic energy during collisions, can take place between ions and neutral atoms of like-species [18]. The use of liquid hydrogen and hydrazine for propellant means hydrogen atoms are released into the space environment and have the ability to interact with other hydrogen particles, resulting in charge exchange and potentially ionization.

Reference [14] performed a simulation of neutral and ionized plume species as emitted from a hydrazine thruster in the approximately 1-N class (based on provided thruster exit velocity and mass flow rate) and found that neutral species generally extend from a thruster into a classical conical shape, with limited expansion of lowest-mass species into the surrounding vacuum. The bulk of neutral plume material becomes a conical plume; a small amount becomes a plume approaching a hemispherical shape with some spread of emitted species forward in the direction of motion of the vehicle, up to approximately the surface of the plane normal to the thrust direction and located directly at the outlet of the thruster - the thruster exit plane. Some lightweight species, specifically in the case of the $H_2$ atoms, scatter forward past the thruster exit plane [14] and assume an amorphous shape. Ionic species, created either by interaction of neutral plume emissions or photoionization, tend to scatter much further forward. The heavier ionic species also can generate amorphous wing shapes; the lighter can scatter sufficiently forward past the engine bell exit plane to nearly surround the entire vehicle.

### 4.2 Observed Hemispherical Plumes

Figures 5, 6, and 7 below depict hemispherical plumes for AFSPC-4, AFSPC-6, and USSF-8 over time from left to right, where each plume lasts between 1 and 3 minutes from expulsion to dissipation. Only certain frames of the entire plume expansion are depicted below. The time signatures are included at the bottom of the images and can be read as 'hour - minute - second.' While the plumes vary in angle, size, and density, they all have relatively similar plume expansion styles, expelling radially outward from the satellite and dissipating rather quickly.

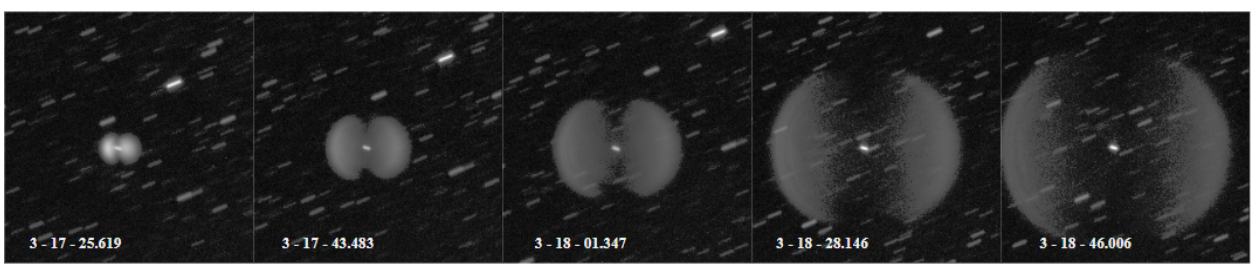


Fig. 5. AFSPC-4 Hemispherical Plume

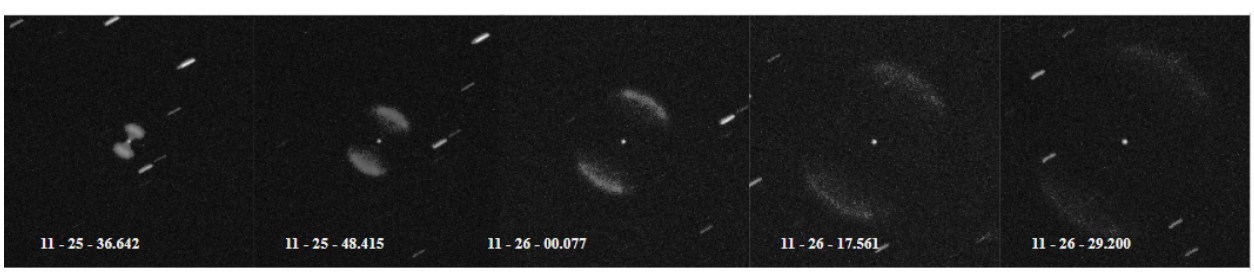


Fig. 6. AFSPC-6 Hemispherical Plume

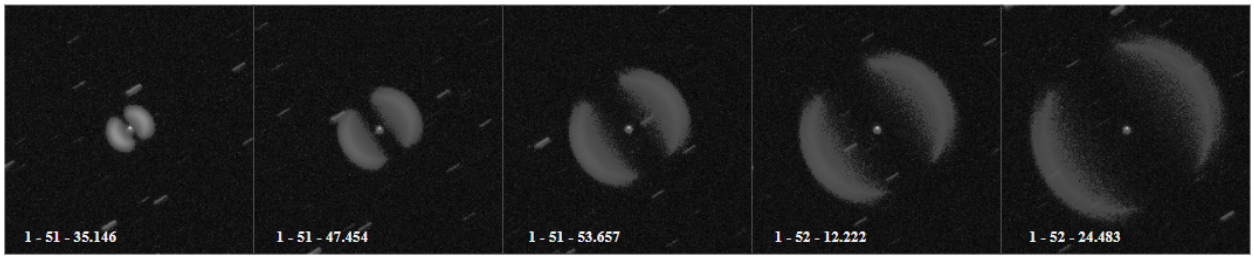


Fig. 7. USSF-8 Hemispherical Plume

From each satellite, the hemispherical plumes occurred both before and after (but usually before) the conical plumes shown in the next section, sometimes on multiple occurrences beforehand. Based on known characteristics, it is likely that these plumes are the result of regular attitude corrections or small station keeping maneuvers [12]. Fig. 8 below shows hemispherical plumes being expelled in bursts. Unlike the plumes above, these only appear to one side of the satellite with a corresponding particle cloud surrounding the spacecraft as well.

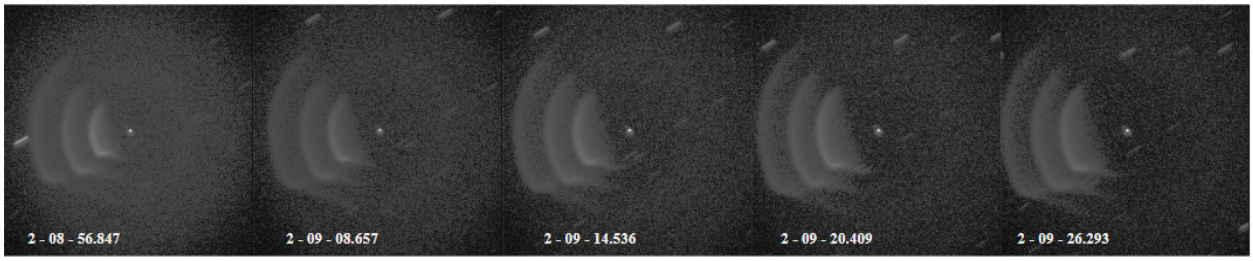


Fig. 8. USSF-8 Hemispherical Bursting Plume

### 4.3 Observed Conical Plumes

On July 29th, 2014 at approximately 06:13:49 UTC, satellite AFSPC-4 was observed to be performing a maneuver, during which a large conical plume appeared to one side of the satellite, shown in the first frame of Fig. 9. The plume remained visible for over 16 minutes. Then a second plume was detected that remained visible in the telescope's Field of View (FoV) for 34 minutes, as shown in frames 2 through 5. The second plume appeared to contain a similar conical core, with a larger amorphous surrounding region.

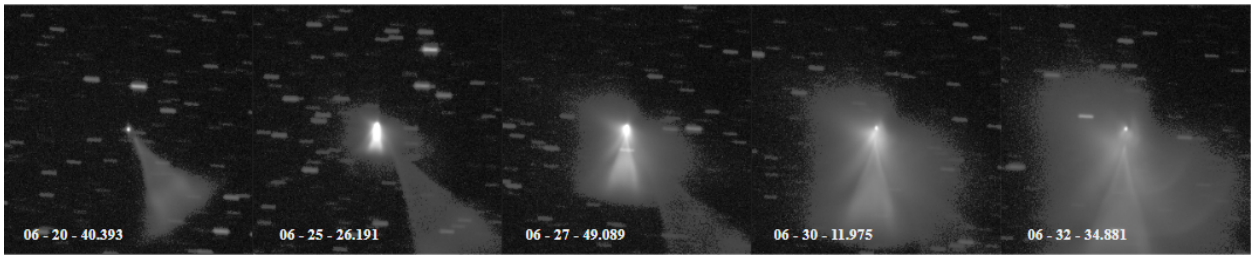


Fig. 9. AFSPC-4 Conical Plume with Amorphous Cloud

Calculations were made to estimate the physical distance of each pixel (distance across an individual pixel) within the sensor's FoV responsible for tracking AFSPC-4. When Exo's sensor data is processed, it is output to an EOD (energy on detector) file format, containing all of the necessary parameters for orbit related calculations. Knowing the range from the sensor to the satellite, and the angle between them, the true distance in real-time 3-D space of each individual pixel can be calculated approximately as 990 meters in the case of AFSPC-4. The pixel length varies for each satellite-sensor combination. The pixel length is necessary for calculating the change in length from tip to base, plume expansion velocity, and plume area which are calculated using equations 1-2. The results are shown in Table 1 below.

Based on known rocket exhaust plume phenomenologies, it is possible these maneuvers are orbital insertion burns or propellant blowdowns [3]. In some situations, the optimal time to perform an orbit insertion maneuver is at apogee. At first glance, they appear to be high impulse maneuvers that expel a large amount of propellant. They also look different from the hemispherical plumes in the previous section. However, it was suggested that the difference in the seemingly separate plumes may merely be a matter of perception. Subsequent investigation was conducted as to whether the conical plumes were the same as the hemispherical plumes just viewed by the sensor at a different orientation. However, the 5th frame of Fig. 9 displays a conical plume having been followed by brief bursts of hemispherical plumes being ejected radially outward, and other captured images not shown contain the same phenomena. The rings of the hemispherical plume are clearly visible, directed toward the bottom right corner of the frame. The significance of this is that both plumes were ejected around the same time without any additional maneuvers or attitude changes in between, nor was the spacecraft believed to have been tumbling. This refutes the idea that the plumes are of the same form being observed at different orientations and instead suggests that the two plumes indeed have a separate set of characteristics and potentially originate from separate propulsion systems.

On August 19th 2016, satellite AFSPC-6 was captured performing a maneuver resulting in conical plume behavior as shown in Fig. 10. The plume, surrounded by a field of propellant particles, remained unchanged in shape or size and within the FoV for over 27 minutes, potentially existing for longer duration**.** In the case of AFSPC-6, the pixel size is roughly 578.5 meters. The previously mentioned calculations were performed for AFSPC-6 and the results are also in Table 1.


Fig. 10. AFSPC-6 Conical Plume with Amorphous Cloud

Finally, on January 22nd 2022, satellite USSF-8 performed a maneuver creating a conical plume, shown in Fig. 11. The expelled propellant remained in its static form for approximately 25 minutes. The pixel distance for this sensor-satellite combination is roughly 613.1 meters. Results from the same calculations are listed in Table 1.

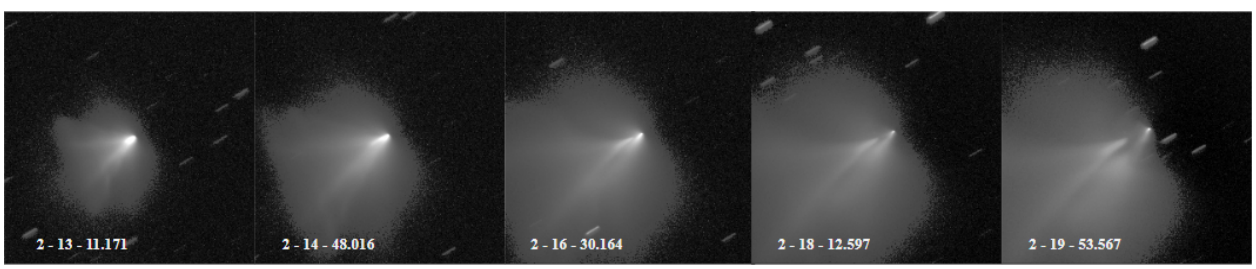


Fig. 11. USSF-8 Conical Plume with Amorphous Cloud

EOD files created by Exo's sensor data were parsed to extract values for calculating a plume's change in length and area over time. Pixel size, or the distance across an individual pixel in terms of physical space, is a necessary value for these calculations. Pixel size is the product of the range, R, between the sensor and the satellite, and the effective instantaneous field of view, α, Eq. (1), where α was first converted from microradians to radians. The range and effective instantaneous FoV measurements are taken from Exo's EOD files and placed with the pixel size calculations in Table 1 for both hemispherical and conical plumes.

$$D_{Pixel} = R * (\alpha * 10^{-6}) \quad (1)$$

To calculate the change in length, L, over time, two frames from the plume image sequence for each satellite were chosen and the lapse in time, ΔT, between them was calculated by subtracting the latter time from the earlier. Then, using an open-source enhanced pixel examiner and basic geometry, the full length from tip of the thruster to the base of the plume was found for each of the two conical plume frames, as well as the full length from the top of the plume to the bottom (relative to the sensor FOV) of the two hemispherical plume frames. The distance of one pixel could then be multiplied by the total number of pixels in a certain measurement to determine the distance in 3-D space. The open-source pixel examiner was chosen for better accuracy as compared to manually counting pixels by hand. The change in length over time was then calculated and listed in Table 1 for both plume types. A similar process was completed to calculate the change in plume cross-sectional area over the chosen elapsed time. Using the change in length (distance of the plume from one end to the other) over time, the equations for area of a triangle and semicircle (to account for 2-D space) were applied to compute the change in area over time for both plume types, Eq. (2, 3). The resulting values are listed in Table 1.

$$\Delta A_{Triangle} = \tfrac{1}{2} * \text{base} * \Delta L \tag{2}$$

$$\Delta A_{Semicircle} = \tfrac{1}{2} * \pi * (\Delta L / 2)^2 \tag{3}$$

Table 1. Satellite Conical and Hemispherical Plume Expansion Calculations

| Satellite | Shape | Range (m) | α (urad) | $D_{Pixel}$ (m) | ΔT (s) | ΔL / ΔT (m/s) | $\Delta A_{Plume}$ ($m^2$/s) |
|---|---|---|---|---|---|---|---|
| AFSPC-4 | Conical | 37,708,400 | 25.49 | 990 | 89.29 | 324 | 10,450,000 |
| AFSPC-4 | Hemisphere | 38,854,140 | 25.49 | 990 | 17.87 | 1,240 | 50,703,000 |
| AFSPC-6 | Conical | 35,434,790 | 16.33 | 578.5 | 134.01 | 258 | 5,266,000 |
| AFSPC-6 | Hemisphere | 38,234,795 | 16.33 | 624.4 | 11.69 | 1,230 | 29,834,000 |
| USSF-8 | Conical | 37,520,070 | 16.34 | 613.1 | 48.81 | 433 | 15,865,000 |
| USSF-8 | Hemisphere | 37,520,135 | 16.34 | 613.1 | 12.40 | 1,509 | 46,978,000 |

These calculations are important in understanding how plumes vary in their expansion and lead to the following questions: What effect does the space plasma environment have on these plume characteristics, if any? Are these plumes behaving as such due to surrounding plasma, propulsion system factors, a combination of both, or something else entirely? These questions will be addressed in subsequent sections.

## 5. EXPLORING PLUME BEHAVIOR

### 5.1 Shape

Solely based on Exo's observations and combined knowledge of previous research, the variation in plumes can be measured and described both qualitatively and quantitatively in terms of what *appears* to be happening; Differences in shape alone suggest separate causes. The hemispherical and conical plumes are named as such because of their physical appearance in 2-D pixel space.

The hemispherical plumes from each of the three satellites all exist in two arced lobes and expand outward away from the source. After the cutoff of upper stage engines, propellant venting and attitude control maneuvers are common. In the presence of extremely low pressure at high altitudes, vented propellant produces a rapidly expanding cloud of particles and vapor due to quick evaporation [3]. Based on findings from [14], this is another possibility for the origin and shape of the hemispherical plume. What is not well understood is *why* the hemispherical plumes are released in two lobes, one from each side of the satellite, or in the interesting case of the bursting plumes, from one side. Publicly available information on satellites is not always complete, and it is possible

that the hemispherical plumes we have observed originate from another set of thrusters on board, such as RCS (Reaction Control System) thrusters that typically use hydrazine. The conical plumes are believed to originate from either the second stage engine before the separation of payload and launch vehicle, or another main thruster on the satellite. We do not have the information to confirm this, however one source describes the necessity of the liquid apogee engine (LAE) for GEO satellites to use during apogee injection and some station keeping maneuvers, and mentions other works that have studied the use of multiple small thrusters for attitude control [10]. This suggests the possibility that the hemispherical plumes may come from other thrusters not described by public information.

The conical plumes from each of the three satellites appear triangular in shape and in the relative 2-D pixel space, originate from a single point and expand as if constrained by boundaries. The reason the conical plume is termed as such is because in 3-D space, it is believed to display a cone-like shape relative to the sensor. Concurrently, one source writes that rocket plumes at extreme altitudes are assumed to expand freely, presenting a conical form as viewed by the sensor, and further explains that at higher altitudes, the ambient densities of the surrounding environment are sufficient enough to somewhat confine the region of reaction [3]. During the entire expansion, and for a time after, the conical plumes move with their associated satellite in its trajectory, whereas the hemispherical plumes do not; in that case, the lobes move away from the thruster. Additionally, there are amorphous gas clouds present in the images of the conical plumes. These have been previously studied [10, 13, 14] and are likely caused by the backflow of the exhaust in the rarefied (less dense than usual) ambient environment as well as the local electrostatic forces causing plumes to expand upstream. This may provide some explanation of the physical nature of the two different plume shapes.

### 5.2 Density

Especially at GEO in a near vacuum environment, plumes that form as a result of high delta-v maneuvers or orbital inclination and injection burns tend to be of high density relative to the local ambient space [14]. This is apparent in Fig. 9, 10, and 11. The conical plumes appear denser in relation to the hemispherical plumes because the stars in the image background are barely visible through the conical plumes. The formation of those high-density plumes is known to be a product of post-combusted neutral particles interacting with ambient space plasma via charge exchange [14]. This would indicate that during high delta-v maneuvers or other highly exhaustive burns, large amounts of neutral-ion collisions take place.

### 5.3 Brightness

The contents of exhaust plumes may also have an effect on its visibility relative to ground-based optics. Images of the Apollo 8 translunar injection burn were captured by a telescope of the Smithsonian Astrophysical Observatory in Maui, Hawaii. One image in particular (Fig. 12) displays a massive conical plume lit by the sun and observed during twilight. From this image, it has been concluded that plume particles must be formed by the rapid expansion of exhaust into the space environment relative to the ambient pressure, and that rapidly cooled condensed water vapor product is responsible for scattering of sunlight [3]. Because some maneuvers from the satellites studied in this paper rely on the combustion of liquid hydrogen with liquid oxygen, water vapor is the main exhaust product. Such scattering due to condensed water vapor may be the reason behind Exo's ability to observe such bright plumes.

As a whole, the water vapor product is not thought to be affected by the plasma environment, but the individual hydrogen and oxygen particles within it are, and their behavior may make the difference between the two types of plumes described in this research. As noted earlier, the highest density areas of the plumes typically occur near the thruster exit, which simultaneously is where scattering is the strongest [14], suggesting why the conical plumes presented in Exo's images are brighter in pixel space than the hemispherical plumes. Another possibility is that the hydrazine used on the possibly-present satellite thrusters does not produce as much scattering after interactions with the charged space environment as combusted water vapor would.

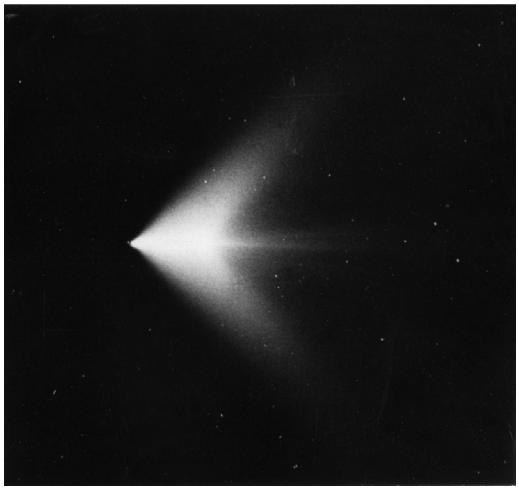

Fig. 12. Apollo 8 Translunar Injection Burn [3, pg. 64]

**5.4 Expansion Velocity and Area Expansion**

Table 1 lists the values of the plume expansion velocity as well as the change in plume area over time in 2-D space. Using frame by frame measurements to calculate the plume expansion, AFSPC-4, AFSPC-6 and USSF-8 produced hemispherical plumes expanding at roughly 1.240 km/s, 1.230 km/s, and 1.509 km/s respectively. They also produced conical plumes expanding at roughly 0.324 km/s, 0.258 km/s, 0.432 km/s respectively. Note that these values reflect how fast the plumes grow over time, not necessarily the velocity of the moving particles exiting the thruster. The values seem reasonable, given that one source describes observed exhausted plume flow velocities in LEO up to 3 km/s for inserting spacecraft [2], and it is likely that after expulsion, the velocity of the plumes and subsequently their growth, would slow. At GEO, orbital speed requirements are lower than at LEO, as well as the velocity required for insertion to such an orbit.

The hemispherical plumes are much greater in their expansion velocity as well as change in area over time as compared to the conical type. This could be due to the hemispherical plumes resulting from short-lived station keeping maneuvers, or possibly the use of smaller thrusters in comparison. In the case of AFSPC-4, the expansion velocity of the hemispherical plume is roughly 3.82 times faster than that of the conical plume. Likewise, the area of the hemispherical plume grows nearly 5 times faster than that of the conical plume after expulsion. During the AFSPC-6 maneuvers, the exit velocity of the hemispherical plume relative to the conical plume can be described by a ratio of 4.76:1, and the change in plume area is calculated to be 5.66:1. Finally, for USSF-8, the exit velocity ratio of hemispherical style to conical is 3.49:1, and the ratio of change, or growth, in area is 2.96. The reason why the ratios for USSF-8 appear to be appreciably smaller is likely because the second stage engine on board is smaller than what is used for the AFSPC satellites, and presumably the other thrusters on board as well.

A pattern is present here. All values for the hemispherical plumes in terms of expansion speed and size are much greater than their conical counterparts. While these factors may not exclusively pertain to interactions with the space plasma environment, they do suggest a difference in propulsion properties.

## 6. PROPULSION SYSTEM PROPERTIES

The properties of the satellites' propulsion systems are important in understanding the characteristics of the expelled plumes. AFSPC-4 and AFSPC-6 both launched on ULA Delta IV rockets and both contain Delta Cryogenic Second Stage (DCSS) engines constructed of various aluminum parts [11]. The satellites are fueled by liquid hydrogen and liquid oxygen and each uses a single RL10B-2 engine shown in Fig. 13. USSF-8 contains a different engine - the Centaur second state engine, equipped with a cryogenic tank and similarly, liquid hydrogen and liquid oxygen for fuel. A list of properties for each engine type is located in Table 2 below. Assuming there are also smaller RCS thrusters on board the satellites, approximate properties for one version of that engine type are also listed in Table 2.

For comparison purposes, the actual model of RCS thrusters does not matter so much here, as the point is to show the considerable difference between properties of the main engines and the smaller thrusters.

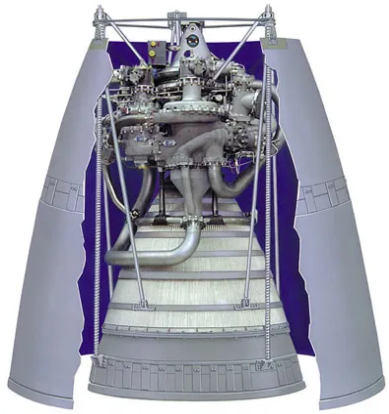

Fig. 13. RL10B-2 Upper Stage Rocket Engine [15]

Table 2: Propulsion System Properties of the RL10B-2 and RL10C-1 Engines

| PARAMETERS | RL10B-2 | RL10C-1 | RCS |
|---|---|---|---|
| **Launch Vehicle** | Delta IV | Atlas V | n/a |
| **Thrust** | 24,750 lbf | 22,890 lbf | 18 lbf |
| **Fuel** | Liquid Hydrogen | Liquid Hydrogen | Dinitrogen Tetroxide ($N_2O_4$) |
| **Oxidizer** | Liquid Oxygen | Liquid Oxygen | Liquid monomethylhydrazine ($CH_6N_2$) |
| **Nominal Mixture Ratio** | 5.88 : 1 | 5.5 : 1 | 2.0 : 1 |
| **Specific Impulse** | 465.5 sec | 449.7 sec | 290 sec |

The combustion of liquid hydrogen and liquid oxygen yields water vapor and energy, shown in equation 4. Knowing that like-species interact in the plasma environment, the neutral hydrogen and oxygen products likely undergo many neutral-ion interactions and charge exchanges with $H^+$ and $O^+$ ions in the ambient GEO environment.

$$2H_2 + O_2 \rightarrow 2H_2O + \text{Energy} \tag{4}$$

In RCS thrusters, the combustion of monomethyl hydrazine and dinitrogen tetroxide yields nitrogen, carbon dioxide, and water vapor shown in equation 5. The post combustion water vapor likely interacts with the ambient plasma environment more than the other products, producing more scattering. One source found that plume dissipation may actually be linked to the species type in the propellant [14], where certain species travel faster across space than others. Reference [14] discovered in their research of modeled hydrazine plumes that the $H_2$ species generally traveled faster than the $N_2$ species, but the $N_2$ species was found to dissipate into ambient density levels first.

$$4CH_3NHNH_2 + 5N_2O_4 \rightarrow 9N_2 + 4CO_2 + 12H_2O \tag{5}$$

Other important factors to consider in classifying plume differences include mass flow rate and exit velocity, among others that will be highlighted in a later section. In this study, it was necessary to first consider the flow of plumes as supersonic. The following assumptions allowed us to apply fundamental nozzle design theory to back out ideal gaseous exit velocity characteristics from publicly available thruster performance parameters: isentropic relations,

ideal gas, and steady 1-D flow. Using data and charts available in [19, 20], the calculated mass flow rate for the RL10B-2 engine using liquid hydrogen and liquid oxygen is 24.13 kg/s and the exit velocity is 4.44 km/s. In the case of an RL10C-1 engine also fueled by liquid hydrogen and oxygen, the calculated mass flow rate is 23.06 kg/s, and exit velocity is 4.25 km/s. Finally, in the assumed presence of RCS thrusters and hydrazine propellant, an estimated mass flow rate and exit velocity are 0.03 kg/s and 2.84 km/s, respectively. At first glance, the calculated values are not so different between the RL10B-2 and RL10C-1 engines, but considerable between them and the RCS thrusters.

A high mass flow rate is associated with both high density and high velocity. Interestingly, calculating plume properties under the ideal gas assumption suggests that plumes from the larger engines should travel and expand faster than plumes expelled from smaller thrusters. What our processed image data shows is counterintuitive in that regard - the conical plumes emitted by the larger engines actually expand at a much slower rate than the hemispherical plumes believed to be emitted by the satellite's RCS thrusters. Possible reasons will be discussed in section 9.

## 7. THE MAGNETIC FIELD AT GEO

It has been established that ions within a plasma react to the presence of magnetic fields, so it is important to understand the extent to which the earth's magnetic field at GEO affects the charged plumes under investigation. References [12, 14] both explain that the magnetic field strength at GEO relative to LEO is much weaker. It is also far less dense but contains higher energies of ambient ions. The magnetic field is far more likely to have an effect on ion plumes and their development than neutral plumes, however, that effect is believed to be minimal and is often ignored in the models from these studies [12, 14].

It was suggested that while the strength of the magnetic field itself may have negligible effects on plumes, perhaps the difference in direction between the satellite's thrust vector and the magnetic field may have an impact. However, in the case of GEO satellites that often remain stationary in the relative sense and whose thrust vectors are perpendicular to the magnetic field lines, once again, there isn't much influence [14]. It is unknown whether or not the satellite thrust vectors of this study are directly perpendicular to the magnetic field lines; it may be possible that deviations can have an effect on plume development relative to the sensor. For better representation, Fig. 14 below depicts the direction of the earth's magnetic field lines at GEO on the respective day and time of the observed plumes. It also incorporates the locations of the satellites (pink dots) relative to the sensors (green dots) detecting them.

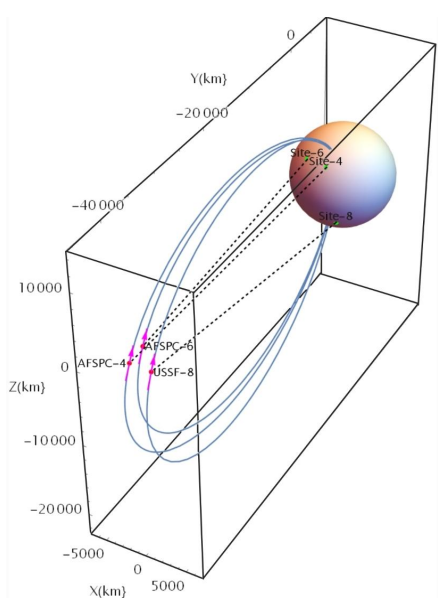


Fig. 14. Geostationary satellites on magnetic field lines relative to associated Exo telescope sites

Note that for this study, effects due to solar storms or large influxes of charged particles by the sun were ignored. Reference [12] found that photoionization (ionization due to photon collisions with other particles) does not have an effect on neutral plume properties.

## 8. MODELED PLUMES

### 8.1 Methodology

Exo has developed software for simulating the fully nonlinear physics of plasmas for applications ranging from fusion research, space weather, and hypersonic wake dynamics. The code base includes MHD, multi-species plasma fluid, PIC, and hybrid fluid/PIC simulations. The suite of codes model electrons and multiple ion species, evolving them in time via the equations below (not an exhaustive list) (Fig. 15), making use of the flux corrected transport routines for advection and a fourth order Runge-Kutta algorithm to evolve source terms. The codes also feature a linearized mode that allows the user to evolve only the perturbations about an equilibrium.

$$\frac{\partial n_i m_i}{\partial t} + \nabla \cdot n_i m_i \vec{u}_i = 0$$

$$\frac{\partial n_i m_i \vec{u}_i}{\partial t} + \nabla \cdot n_i m_i \vec{u}_i \vec{u}_i + \nabla p_i = n_i q_i (\vec{E} + \vec{u}_i \times \vec{B})$$

$$\frac{\partial \varepsilon_i}{\partial t} + \nabla \cdot (\vec{u}_i p + \vec{u}_i \varepsilon_i) = n_i q_i \vec{u}_i \cdot \vec{E}$$

$$\frac{\partial \vec{B}}{\partial t} = -\nabla \times \vec{E}$$

$$\frac{\partial \vec{E}}{\partial t} = c^2 \nabla \times \vec{E} - \vec{J} / \varepsilon_0$$

Fig. 15. Multi-fluid equations used for MHD and PIC models

For this initial effort, a simpler simulation was created from hot exhaust gas expanding into a low-density background gas to represent spacecraft plumes injecting into the low-density ambient space environment. This model is an examination of the nature of non-ionized plumes that can be treated as an ideal gas, and as such is a means to understand whether or not the observed plume behavior can be reasonably explained. The simulation was run with several parametric variations of velocity of the exhaust gas while pressure and density remained constant. Initial results are shown in Fig. 16 below.

### 8.2 Results and Discussion

Running the simulation given the conditions above results in conically expanding plumes of various shapes. The key parameter that determines the character of the exhaust gas expansion in the model is the ratio of the thermal speed to the exhaust speed. Ideally, the shape of the expansion can be parametrized in terms of the ratio of the pressure (proportional to the thermal speed squared) and the kinetic energy density (proportional to the exhaust velocity squared) of the exhaust. In the plots shown below, the ratio of the exhaust velocity to thermal velocity is 2, 5, and 10 from left to right. Velocity ratios higher than 10 were not selected for this model due to increasingly long run-times.

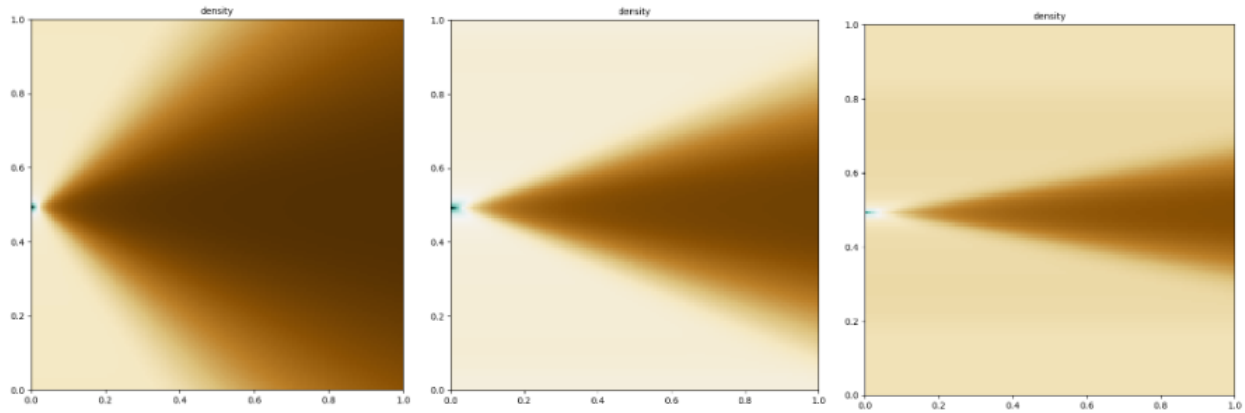


a. Plume density at $V_e/V_t = 2$ b. Plume density at $V_e/V_t = 5$ c. Plume density at $V_e/V_t = 10$

Fig. 16. Conical plumes in a low-density environment under various exhaust velocity conditions

The model illustrates that as the ratio of exhaust velocity to thermal velocity increases, the conical shape becomes smaller and less dense. Based on these results, a conical plume appears to be a product of a neutral, non-ionized gas expansion and is able to be represented well without further modeling. The propulsion properties calculated under the ideal gas assumption from section 6 would agree with the results of this model, in that conical plumes emitted by large engines should have a higher exit velocity and be less dense than the hemispherical plumes being ejected by smaller thrusters at a lower exit velocity. This means some ejected propellant plumes can indeed be modeled as non-ionized heated gasses.

Interestingly, however, the observations in this study have been found to exhibit contrary behavior to both the model and ideal nozzle calculations. The observations and values from Table 1 indicate that conical plumes are denser and expand at much lower velocities than hemispherical plumes that are actually far less dense and expand rapidly. In general, the approach in this section appropriately simulates neutral conical plumes, but at GEO propellant interactions with the plasma environment are far from equilibrium. For example, the amorphous clouds often observed surrounding large conical plumes are believed to originate from ionization mechanisms, something the current model does not illustrate. These observations illuminate that fluid dynamics alone is insufficient in determining complex plume development and behavior, thus further investigation is necessary.

Future directions of the simulations will include a background magnetic field with both MHD and multi-fluid fully ionized plasma treatments of the exhaust to develop intuition of the sensitivities of the exhaust dynamics as the particles of propellant plumes become ionized. Longer term plans include particle-in-cell simulations.

## 9. CONCLUSIONS

This paper published image data showing optically-detected plumes from several events wherein plumes were generated. Three varieties of plume shape (conical, hemispherical, and amorphous) were shown, described, and initially characterized. Upon closer examination, hemispherical and conical plumes were discovered to share a pattern, in that both types of plumes were seen to be emitted by all of three exemplar plume-emitting vehicles (generally hemispherical, followed by conical), and the rates of change in length and change in area over time between the two types were approximately similar across all three vehicles - that is, a hemispherical plume grows roughly 3 to 5 times as quickly as a conical plume.

This consistent pattern points at a possible relationship between plume types and thruster types. We may suppose that smaller thrusters (which generally use hydrazine) tend to produce hemispherical plumes, while larger thrusters (especially those using LOX/LH2 to produce water vapor) may tend to produce conical plumes. If it can be further validated in future work, this relationship may be used to determine from optical imagery the type of thrusters being activated by a space vehicle during a given observed maneuver. Furthermore, as it is also possible that the amorphous plume shapes which attend conical plumes are produced as a result of particles in a conical plume becoming ionized and spreading forward of the engine exhaust plane, it may be possible to analyze the rates and

extent of plume spread from conical to amorphous and derive possible combustion properties, such as precise propellants used or mixture ratios applied.

Initial investigation of possible relationships between the magnetic field and spacecraft did not immediately suggest apparent interaction effects, although interaction also cannot be ruled out. The simple fact that three spacecraft in the GEO neighborhood were each seen to produce multiple varieties of plume, sometimes nearly contemporaneously, suggests that magnetic field lines are not a primary driver of observed behavior, as the relationship between said field lines and the motion and position of a spacecraft in GEO does not alter greatly in short (or, when at GEO, comparatively long) periods of time.

Although a fully modeled analysis of complex interactions among solar flux, the Earth's magnetic field lines, other propulsions properties such as total delta-v and the relative velocity between a spacecraft and its propellant plume, as well as the local plasma environment is beyond the scope of this paper, a key direction for future work will be performing in-depth modeling of the relationships among these elements.

## ACKNOWLEDGEMENTS

The authors would like to thank Dr. Paul Bernhardt from the University of Alaska for his technical insight, guidance, and contribution of key figures and concepts to this work.

## REFERENCES

[1] Chen, Francis F., 1929-. *Introduction to Plasma Physics and Controlled Fusion*. New York: Plenum Press, 1984.

[2] Bernhardt, Paul A., et al. Satellite observations of strong plasma wave emissions with frequency shifts induced by an engine burn from the Cygnus spacecraft. *Radio Science*, vol. 56, no. 2, 2021.

[3] Simmons, Frederick S., 2000-. *Rocket Exhaust Plume Phenomenology.* El Segundo, The Aerospace Press, 2000.

[4] Tsurutani, Bruce T., et al. Space Plasma Physics: A Review. *arXiv.Org*, 29 Sep. 2022.

[5] Stephani, K. A., Boyd, I. D., Balthazor, R. L., McHarg, M. G., Mueller, B. A., and Adams, R. J., Analysis and Observation of Spacecraft Plume / Ionosphere Interactions During Maneuvers of the Space Shuttle, *Journal of Geophysical Research*: *Space Physics*, Vol. 119, No. 9, 2014, pp. 7636–7648.

[6] Denton, M. H., M. F. Thomsen, H. Korth, S. Lynch, J. C. Zhang, and M. W. Liemohn (2005), Bulk plasma properties at geosynchronous orbit, *J. Geophys. Res.*, 110, A07223

[7] Gallagher, Dennis L. The Earth's Plasmasphere. *NASA*, NASA, 2015, plasmasphere.nasa.gov/formed.html.

[8] Carreau, C. Earth's Plasmasphere and the Van Allen Belts. *Cluster*, European Space Agency, 10 Sept. 2013.

[9] Yue, C., Bortnik, J., Li, W., Ma, Q., Gkioulidou, M., Reeves, G. D., et al.(2018). The composition of plasma inside geostationary orbit based on Van Allen Probes observations. *Journal of Geophysical Research: Space Physics*, 123, 6478–6493

[10] Kyun Ho Lee, Plume simulation of liquid apogee engine for GEO satellite using parallel DSMC method, *Computers & Fluids*, Volume 208, 2020, 104612, ISSN 0045-7930..

[11] Delta IV AFSPC-4 Mission. United Launch Alliance, 2014. PDF file.

[12] Weaver, Andrew B., and Iain D. Boyd. Unsteady simulations of Rocket Plume expansions in Geostationary Earth orbit. *Journal of Spacecraft and Rockets*, vol. 54, no. 6, 2017, pp. 1258–1266.

[13] Machuzak, John S., et al."Effects of thruster firings on the Shuttle's plasma and Electric Field Environment. *Journal of Geophysical Research: Space Physics*, vol. 98, no. A2, 1993, pp. 1513–1530.

[14] Stephani, K. A., and I. D. Boyd (2016), Spacecraft plume interactions with the magnetosphere plasma environment in geostationaryEarth orbit, *J. Geophys. Res.Space Physics*,121, 1402–1412.

[15] RL10B-2. *AeroSpaceGuide.Net*, 4 July 2017, www.aerospaceguide.net/rocketengines/RL10B-2.html.

[16] Matéo-Vélez, J.-C., et al. Spacecraft surface charging induced by severe environments at geosynchronous orbit. *Space Weather*, vol. 16, no. 1, 22 Dec. 2017, pp. 89–106.

[17] Boyd, I. D., and A. Ketsdever. Interactions between spacecraft and thruster plumes. *Journal of Spacecraft and Rockets*, vol. 38, no. 3, 2001, pp. 380–380.

[18] Frank-Kamenetskii, D.A. *Collisions with Neutral Particles*. In: Plasma. Palgrave, London. 1972.

[19] Humble, R.W., G. N. Henry, and W. J. Larson. *Space Propulsion Analysis and Design*. 1st ed. rev. New York: McGraw-Will, 1995

[20] Sutton, G. P. and O. Biblarz. *Rocket Propulsion Elements*. 9th ed. Hoboken, New Jersey: Wiley, 2017.